Global mean surface temperature response to large-scale patterns of variability in observations and CMIP5

Jules B. Kajtar[1], Matthew Collins[1], Leela. M. Frankcombe[2,3], Matthew H. England[2,3], Timothy J. Osborn[4], Marcus Juniper[1]

[1] College of Engineering, Mathematics, and Physical Sciences, University of Exeter, Exeter, UK.

[2] Australian Research Council's Centre of Excellence for Climate Extremes, Australia.

[3] Climate Change Research Centre, University of New South Wales, NSW, Australia.

[4] Climatic Research Unit, School of Environmental Sciences, University of East Anglia, Norwich, UK.

Corresponding author: Jules B. Kajtar (j.kajtar@exeter.ac.uk)

Key Points:

- Interdecadal Pacific Oscillation and Atlantic Multidecadal Variability are weaker than observed in state-of-the-art models.
- Correlations between these patterns and global temperature changes are identified, but these too are weaker in models.
- Models that exhibit stronger variability in these patterns also exhibit stronger relationships between the patterns and global temperature.

Abstract

Global mean surface temperature (GMST) fluctuates over decadal to multidecadal time-scales. Patterns of internal variability are partly responsible, but the relationships can be conflated by anthropogenically-forced signals. Here we adopt a physically-based method of separating internal variability from forced responses to examine how trends in large-scale patterns, specifically the Interdecadal Pacific Oscillation (IPO) and Atlantic Multidecadal Variability (AMV), influence GMST. After removing the forced responses, observed variability of GMST is close to the central estimates of Coupled Model Intercomparison Project Phase 5 (CMIP5) simulations, but models tend to underestimate IPO variability at time-scales >10 years, and AMV at time-scales >20 years. Correlations between GMST trends and these patterns are also underrepresented, most strongly at 10- and 35-year time-scales, for IPO and AMV respectively. Strikingly, models that simulate stronger variability of IPO and AMV also exhibit stronger relationships between these patterns and GMST, predominately at the 10- and 35-year time-scales, respectively.

Plain Language Summary

Despite the smooth and steady increase of greenhouse gas concentrations, the rate of global warming has not been as stable over the past century. There are periods of stronger warming, or even slight cooling, in the global mean temperature record, which can persist for several years or longer. These changes have been linked to regional climate patterns, most notably within the Pacific and Atlantic Ocean climate systems. Climate models do not exhibit the same level of variations in these Pacific and Atlantic oscillations as compared to the observed record, and the connections between these oscillations and the global temperature are also diminished. However,

there is a tendency for those models that show stronger Pacific and Atlantic oscillations to also exhibit stronger relationships between these patterns and global temperature changes.

1 Introduction

Anthropogenic greenhouse gases have been responsible for global warming over the last century, but a range of drivers have contributed to variations in the observed global mean surface temperature (GMST) across a range of time-scales. The slowdown in global warming during the early 21st Century, sometimes referred to as the "hiatus", has garnered extensive research. Numerous mechanisms have been proposed for the slowdown (see Medhaug et al. 2017 for a comprehensive review), but many argue that particular patterns of internal climate variability drove the weaker GMST trend. For example, the negative phase of the Interdecadal Pacific Oscillation (IPO) appears to have played a role in the slowdown (Kosaka & Xie 2013; England et al. 2014; Watanabe et al. 2014), and the strength of the negative IPO may have in part been enhanced by a strong Atlantic warming trend (McGregor et al. 2014; Chikamoto et al. 2016; Li et al. 2016).

The association of the global warming slowdown with internal variability has motivated this study on the extent to which large-scale patterns of variability drive decadal or multi-decadal trend changes in GMST, in both observations and models. The common view is that the Pacific Ocean plays a substantial role in modulating GMST. As already noted, the IPO is thought to be tied to decadal-scale GMST trend changes (England et al. 2014; Maher et al. 2014; Dai et al. 2015; Kosaka & Xie 2016; Meehl et al. 2016; Henley & King 2017). However, Atlantic

Multidecadal Variability (AMV) has also been linked with GMST changes (Mann et al. 2014; Chylek et al. 2016; Pasini et al. 2017; Wang et al. 2017), as have the AMV in combination with Pacific variability (Dong & Zhou 2014; Steinman et al. 2015; Yao et al. 2016; Nagy et al. 2017; Stolpe et al. 2017). The Indian (Luo et al. 2012) and Southern Oceans (Oka & Watanabe 2017) may also play a role. This study focusses on the two dominant patterns of internal variability at decadal and multi-decadal time-scales: the IPO and AMV.

Central to the analysis of GMST variations is the separation of internal variability and forced response. The simplest method of excluding the anthropogenic greenhouse gas forcing signal is to remove a linear trend, but this introduces spurious signals, as the forced response is not linear (Mann et al. 2014; Frankcombe et al. 2015). Another approach is to subtract a global mean sea surface temperature (SST) time-series (e.g. Trenberth & Shea 2006; Douville et al. 2015; Farneti 2017; Lyu & Yu 2017), but again this is problematic, since it removes a component of desired internal variability. In this study, an approach based on the response in multiple model simulations is adopted (Allen & Stott 2003; Schurer et al. 2013; Mann et al. 2014; Frankcombe et al. 2015; Steinman et al. 2015). This approach removes an estimate of responses to forcings that are common across the model ensemble, i.e. anthropogenic greenhouse gas and aerosol forcing, as well as volcanic aerosol forcing.

With an estimate of the forced response removed, the performance of the Coupled Model Intercomparison Project Phase 5 (CMIP5) historical experiments in simulating the observed variability in GMST, the IPO, and AMV, at a range of inter-decadal to multi-decadal time-scales

89 is assessed. Correlations are then computed between these three indices, again at a range of time-
90 scales, to determine the extent to which large-scale patterns of variability may imprint on GMST.
91
92 **2 Data**
93
94 The analysis of GMST, IPO, and AMV is conducted over the period 1880 to 2017. The
95 HadISST v1.1 sea surface temperature (Rayner et al. 2003) is analyzed together with the
96 HadCRUT v4.5.0.0 surface air temperature (Morice et al. 2012). The observed relationships are
97 compared to the historical simulations in CMIP5. Most historical simulations were run to 2005,
98 and thus they are extended here to 2017 with the RCP8.5 (representative concentration pathway;
99 Riahi et al. 2011) simulations. The choice of RCP extension does not make a significant
100 difference for the early period of the 21st century (e.g. Collins et al. 2013; England et al. 2015).
101 The two CMIP5 variables analyzed herein are SST (CMIP5 variable name: *tos*), and surface air
102 temperature (*tas*). The available ensemble members are listed in Table S1.
103
104 The IPO is characterized by the tri-polar index (TPI; Henley et al. 2015), defined as
105 $\mathrm{TPI} = T_C - \frac{1}{2}(T_N + T_S)$, where the terms represent SST area-averages over the central Pacific,
106 T_C: $10°\mathrm{S} - 10°\mathrm{N}, 170°\mathrm{E} - 90°\mathrm{W}$, the north Pacific, T_N: $25° - 45°\mathrm{N}, 140°\mathrm{E} - 145°\mathrm{W}$, and the
107 south Pacific, T_S: $50° - 15°\mathrm{S}, 150°\mathrm{E} - 160°\mathrm{W}$. AMV is represented by the area-averaged SST
108 over the North Atlantic region of $5° - 60°\mathrm{N}, 80°\mathrm{W} - 10°\mathrm{W}$ (Knight 2009). GMST is simply the
109 global weighted average of surface air temperature. Blended air and sea surface temperatures
110 (Cowtan et al. 2015) were also tested, but these made negligible differences to the findings.
111

3 Methods

Removing the externally forced response from the data is a key component of this study, so that the patterns of internal variability can be accurately identified. A method based on "optimal fingerprinting" is used (Allen & Stott 2003; Schurer et al. 2013; Mann et al. 2014; Frankcombe et al. 2015, 2018; Steinman et al. 2015). In this approach, the forced response is estimated from an ensemble of model experiments, following the single-factor scaling method of Frankcombe et al. (2015). Details are given in the supporting information (Text S1). Our approach differs from Frankcombe et al. (2015) and Allen & Stott (2003) in that the estimated forced signal is always taken to be the multi-model mean of the CMIP5 historical GMST (Figure S1a; black curve), regardless of whether removing the forced response from an SST index, grid-point SST data, or GMST. The multi-model mean GMST is scaled before subtraction from the raw time-series in each model simulation and the observations (Text S1).

Several choices could have been made in the forced response removal process (Text S1), but ultimately there is no perfect method for the analysis of multiple model simulations together with observations. The simplest approach in this regard has been adopted here, which is to treat each realization independently. However, the approach here is nevertheless a substantial improvement over linear or quadratic detrending (Mann et al. 2014; Frankcombe et al. 2015; Steinman et al. 2015).

Another caveat to this analysis is that the real-world forcings for 2006-2017 have turned out to be different to those applied to the RCP8.5 experiments which were used to extend the

historical simulations to 2017 (Schmidt et al. 2014). For example, the forecast of volcanic forcing, which is thought to be a component driving the early 2000s global warming slow-down, was too weak in the RCP scenarios (Vernier et al. 2011; Huber & Knutti 2014; Santer et al. 2014; Smith et al. 2016). Therefore, the multi-model mean forced signal for the period following 2006 may not deliver the best estimate for the analysis of the observed record. This effect is nevertheless small, especially since the period of analysis stretches back to 1880.

The following analysis is largely of multi-year running-trends (Text S2) of annual mean data (Figure S1a-c) after the forcing response has been removed (Figure S1d-f). All quoted values of correlations are the Pearson's linear correlation coefficient.

4 Results

4.1 Standard deviation of GMST, IPO, and AMV trends

We inspected the standard deviation of running trends of GMST, and the IPO and AMV indices, over a range of time-scales (Figure 1a-c). Here, and from this point on, the forced response has been removed from all time-series. Although there is a large range in the standard deviation of simulated GMST trends, the observed standard deviations are close to the multi-model mean values across most time-scales (Figure 1a; Flato et al. 2013; Marotzke & Forster 2015). The model-mean standard deviation is slightly larger than in observations for ~5- to 15-year running trends, but nevertheless the observations lie within the central 68% of the model range for all time-scales. Larger differences are seen for the IPO and AMV. For the IPO, the

observations diverge from the model-mean at >10-year running trends (Figure 1b). Beyond 20-year trends, the observed standard deviation is stronger than in a substantial proportion of models, lying well outside the central 68% model range. These findings are consistent with Henley et al. (2017). Standard deviation of AMV index trends in observations and models show better agreement for 10-year trends, but again, observed standard deviation is larger at longer time-scales (Figure 1c; though the standard deviations become more uncertain for these longer windows as there are fewer independent trends). Unlike the observations, the standard deviation across models tend to diminish for longer running trends (in agreement with Cheung et al. 2017).

There is debate in the literature surrounding the origins of AMV. The common view is that AMV is driven mainly by processes internal to the Atlantic climate system, but recent studies reported evidence that external forcing, such as anthropogenic aerosol emissions, also have an influence (see Vecchi et al. 2017 for a summary of these view and supporting references) . To test whether the process of removing the forced response also removes a component of AMV, the piControl experiments were analyzed, after accounting for model drift (Text S1; Sen Gupta et al. 2013). Following the present procedure of forced response removal in the historical experiments, no systematic change in variance is seen across the model realizations in either the 10-year IPO or 35-year AMV running trends (Figure S2a,b). This result conflicts with Murphy et al. (2017), who argue that historical forcings have enhanced AMV. However, their method of linearly detrending the historical simulations is known to create spurious variability (Mann et al. 2014; Frankcombe et al. 2015; Steinman et al. 2015).

4.2 Correlations between GMST, IPO, and AMV trends

To test the influence of large-scale patterns of variability on GMST, correlations were computed between the running trends of GMST and the IPO and AMV indices (Figure 1d,e). Almost all models simulate positive correlations between GMST and IPO trends, in agreement with observations, at shorter time-scales (< 25-trends, Figure 1d), and between GMST and AMV trends at all time-scales. Correlations of annual data in 31-year sliding windows also show that the relationship tends to be positive across models (Figure S2c,d). This finding appears to be inconsistent with Douville et al. (2015; their Figure 1c,d), who show a larger spread of positive and negative sliding correlations across models, for GMST with both Pacific Decadal Oscillation (PDO) and AMV. Douville et al. (2015) analyze PDO, but the difference between the PDO and IPO indices is small (Henley et al. 2015; Newman et al. 2016). The difference between our result and theirs highlights the need for more careful removal of the forced signal from observations and models. The biggest difference in procedures comes from their subtraction of each individual ensemble's global mean SST time-series (rather than the multi-model mean). That step is avoided here because it is specifically those imprints of the large-scale patterns onto the global mean that are sought.

The observed relationship between GMST and IPO trends lies within the central 68% of the model spread, and the model-mean captures the diminishing correlation over longer time-scales (Figure 1d). The GMST and IPO trend correlation peaks near the 10-year time-scale in observations. Despite a statistically significant correlation for 10-year trends in more than 80% of model realizations, that same correlation maximum is not seen in most models. The strongest correlation occurs for 5-year trends in 70% of realizations, and only two simulations exhibit a maximum correlation over 8-to-18-year time-scales. A robust relationship between 10-year

trends of GMST and IPO is also seen in the piControl CMIP5 simulations, where an IPO-like pattern emerges for the strongest cooling and warming decades (Middlemas & Clement 2016).

Observed correlations in trends of GMST and AMV also lie within the central 68% model spread, but in this case the relationships do not diminish over longer time-scales (Figure 1e). For observations, the strengthening of the GMST and AMV trend correlation may be a reflection of stronger AMV at longer time-scales (Figure 1c). Although the multi-model mean correlation does not increase with time-scale as strongly as it does in observations, the slight increase is nevertheless surprising, since the standard deviation of AMV tends to diminish with time-scale in models (Figure 1c).

4.3 Inter-model relationships between GMST, IPO and AMV

Here we explore whether there is any tendency for models simulating stronger IPO or AMV to also simulate stronger correlations with GMST. Analysis of 10-year trends for the IPO (Figure 2a), and 35-year trends for AMV (Figure 2b), suggests that indeed such relationships exists. The "inter-model correlation" is defined as the correlation across all of the available CMIP5 realizations between the index trend standard deviation (data shown in Figure 1b,c), and the correlation between trends in that index and GMST (data shown in Figure 1d,e). The inter-model correlation is 0.77 for the 10-year IPO trends (Figure 2a), and 0.53 for the 35-year AMV trends (Figure 2b). Both values are statistically significant above the 99% confidence level, implying that there is an overall tendency for models simulating stronger IPO at the 10-year time-scale to also simulate a stronger relationship between IPO and GMST trends at that time-scale, and likewise for AMV at the 35-year time-scale.

229

230 The inter-model correlation may also be interpreted as a measure of the extent to which
231 the patterns of variability "imprint" on GMST across the models. We next explored whether
232 strong imprints of IPO and AMV onto GMST exist at all time-scales (Figure 2c,d). The 10-year
233 inter-model IPO imprint on GMST is indicated by a vertical line in Figure 2c (correlation of 0.77
234 in Figure 2a). Similarly, the 35-year inter-model AMV imprint on GMST is indicated by a
235 vertical line in Figure 2d (correlation of 0.53 in Figure 2b). The strongest inter-model
236 correlations emerge at those particular time-scales, i.e. decadal for the IPO, and multi-decadal for
237 AMV. Surprisingly, these tend to be the same time-scales at which the IPO and AMV are
238 strongest in observations, but not necessarily within all nor most models.

239

240 Despite the model underrepresentation of decadal IPO and multi-decadal AMV, there is
241 good agreement between observed and modeled standard deviation of GMST trends (Figure 1a).
242 The inter-model correlations would then appear to imply that if the models simulated more
243 realistic IPO and AMV, they might then overrepresent GMST variability. To explore this
244 discrepancy further, the sensitivity of GMST trends to IPO and AMV trends was tested (Figure
245 2e,f). Although the IPO standard deviation and GMST-IPO correlation are both stronger for 10-
246 year trend data in observations, the sensitivity of GMST to IPO trends is weaker (exhibited by
247 the slopes of ordinary least-squares fits; Figure 2e). The result is similar, but clearer, for AMV
248 (Figure 2f). In observed 35-year trends, a 1°C year^{-1} trend in AMV corresponds with a 0.35°C
249 year^{-1} trend in GMST (i.e. $B = 0.35$ °C per °C). Across all of the model data, $B = 0.54$.
250 Therefore, the overly strong sensitivity of 35-year GMST trends to AMV trends in models
251 appears to play some role in offsetting their weaker standard deviation in AMV trends, thus

252 resulting in GMST variability in the model-mean that is close to the observed. It is unlikely that
253 AMV sensitivity across models is solely responsible for the simulation of GMST trend
254 variability similar to the observations, as the spatial patterns of correlations in the following
255 section will show.
256
257 **4.4 Spatial maps of GMST and SST correlations**
258
259 Spatial correlations patterns between GMST trends and grid-point SST trends can help to
260 identify the regions of strongest bias (Figure 3). Again, it is emphasized that this analysis is
261 conducted with the forced signal removed from GMST and from each SST grid-point. The
262 familiar IPO-like patterns emerge at the 10-year trend time-scale for both observations (Figure
263 3a) and in the multi-model mean of the correlations (Figure 3b). The weaker negative signatures
264 in the North and South Pacific of the model pattern may explain the weaker-than-observed
265 correlation between 10-year GMST and IPO index trends in the multi-model mean (Figure 1d).
266 For 35-year trends, there are more striking differences between the observations (Figure 3e) and
267 the model-mean (Figure 3f). The strong positive correlation signal in the North Atlantic in
268 observations (Figure 3e) is indicative of the relationship revealed in the AMV index analysis
269 (Figure 1e). Although the model-mean also exhibits positive correlations in the North Atlantic
270 (Figure 3f), the global spatial pattern is more notably characterized by a strong positive signature
271 across the tropics. To indicate the model spread in the correlations, the 16^{th} and 84^{th} percentiles
272 (corresponding to the bounds of one standard deviation), computed at each grid-point from the
273 CMIP5 ensemble set, are also shown (Figure 3c,d,g,h). The positive correlations across the
274 tropics for 35-year trends are exhibited by at least the central 68% of simulations (Figure 3g,h).

The multi-model mean correlation patterns of the CMIP5 piControl experiments are very similar to those in historical (Figure S3), which also provides some evidence that the forced response has been removed appropriately from the historical data. The spatial correlation patterns suggest that different processes are responsible for driving GMST trend changes at the multi-decadal time-scale across models and observations (Palmer & McNeall 2014). The multi-decadal North Atlantic influence on global climate is robust in observations (Mann et al. 2014; Chylek et al. 2016; O'Reilly et al. 2016; Wang et al. 2017), but GMST may respond more strongly to multi-decadal tropical variability in models (Figure 3f).

5 Conclusions

After the removal of a reasonable estimate of the forced response, robust relationships between global mean surface temperature (GMST) changes and large-scale patterns of internal variability were found in observed data. GMST trends are most strongly correlated with trends in the Interdecadal Pacific Oscillation (IPO) on decadal time-scales, and with Atlantic Multidecadal Variability (AMV) trends on multidecadal time-scales. The range of standard deviations of GMST trends in CMIP5 historical simulations, also after forced response removal, are close to centered on the observations. However, models tend to exhibit weaker-than-observed standard deviation in IPO index trends at time-scales of >10-years, and in AMV index trends at time-scales of >20-years.

Observed correlations of GMST with IPO and AMV lie within the central 68% model spread, but the multi-model mean is weaker than observed at some time-scales. The largest

difference occurs at the ~10-year time-scale for the IPO-GMST relationship, and at the ~35-year time-scale for the AMV-GMST relationship. However, it was found that models simulating stronger IPO or AMV, tend to also exhibit stronger correlations between GMST and IPO or AMV. Strikingly, the inter-model correlations are the strongest at the 10- and 35-year time-scales. I.e., models that show stronger standard deviation in 10-year trends of the IPO index, tend to also show stronger correlations with GMST trends at that time-scale. Likewise, models with greater standard deviation in 35-year trends of the AMV index tend to have stronger correlations between GMST and AMV trends.

An apparent paradox arises in this study: models underrepresent IPO and AMV, but multi-model mean GMST variability is close to observations across all time-scales. At longer time-scales, it was found that the underrepresentation of AMV in models is offset by stronger sensitivity of GMST to AMV, as compared to observations, thus providing a possible explanation for the discrepancy.

Apart from uncertainties related to the forced response removal, there are additional uncertainties related to this analysis. Firstly, uncertainties in observed SSTs are larger prior to the satellite era, and increasingly so deeper in time (Huang et al. 2018). The conclusions drawn herein are consistent with other observational data-sets, namely GISTEMP (Hansen et al. 2010; GISTEMP Team 2018) and ERSST.v5 (Huang et al. 2017), and also when the analysis is restricted to 1950-2017, a period for which the observational data is more robust (Figure S4). Another potential uncertainty arises in the use of an area-average SST index to characterize the IPO, rather than, say, Empirical Orthogonal Functions. The fixed location SST index may not

accurately capture the IPO in models if their centers of action are slightly displaced spatially, relative to the observations. While the multi-model mean of the GMST correlations with grid-point SST suggest that the IPO pattern overall agrees well with the observed (Figure 3a,b), this could be due to aliased variability in the pattern across the models (Henley et al. 2017).

Despite the robust relationships that have been revealed, it is not possible to infer from correlations alone whether the IPO and AMV are independent drivers of changes in GMST trends, or a response to, for example, top of atmosphere flux variations, or deep ocean changes (Hedemann et al. 2017). Further analysis is also required to identify the model biases that lead to weaker-than-observed IPO and AMV. However, spatial patterns of correlations suggest that different processes are responsible for driving GMST changes at multi-decadal time-scales across models and observations. In the model-mean, multi-decadal GMST trends are more strongly correlated with SST trends in the tropics. Newman et al. (2016) find that linkages between the tropics and the PDO are different in observations and models, perhaps due to El Niño-Southern Oscillation model biases. Biases in simulations of AMV might be linked with underestimated variability in modelled Atlantic Meridional Overturning Circulation (Yan et al. 2018). Additionally, biases in cross-basin interactions may also contribute to diminished variability (McGregor et al. 2018; Kajtar et al. 2018). Nevertheless, this study provides a reasonable starting point for further efforts to identify biases that hamper simulations of large-scale variability.

Acknowledgments and Data

This work was supported by the Natural Environment Research Council (SMURPHS project, NE/N005783/1 and NE/N006348/1). LMF was supported by the Australian Research Council (DE170100367). LMF and MHE were supported by the Australian Research Council's Centre of Excellence for Climate Extremes (CE17010023). We acknowledge the World Climate Research Programme's Working Group on Coupled Modelling, which is responsible for the Coupled Model Intercomparison Project (CMIP), and we thank the climate modelling groups for producing and making their model output available (http://pcmdi9.llnl.gov). We also thank the providers of the following observational datasets: HadISST v1.1 (https://www.metoffice.gov.uk/hadobs/hadisst), HadCRUT v4.5.0.0 (https://crudata.uea.ac.uk/cru/data/temperature), ERSST v5 (https://www.esrl.noaa.gov/psd/data/gridded/data.noaa.ersst.v5.html), and GISTEMP (https://data.giss.nasa.gov/gistemp/).

References

Allen MR, Stott PA. Estimating signal amplitudes in optimal fingerprinting, part I: theory. *Clim Dyn* **21**, 477–491 (2003)

Cheung AH, Mann ME, Steinman BA, et al. Comparison of Low Frequency Internal Climate Variability in CMIP5 Models and Observations. *J Clim* **30**, 4763–4776 (2017)

Chikamoto Y, Mochizuki T, Timmermann A, et al. Potential tropical Atlantic impacts on Pacific decadal climate trends. *Geophys Res Lett* **43**, 7143–7151 (2016)

Chylek P, Klett JD, Dubey MK, Hengartner N. The role of Atlantic Multi-decadal Oscillation in the global mean temperature variability. *Clim Dyn* **47**, 3271–3279 (2016)

Collins M, Knutti R, Arblaster JM, et al. Long-term Climate Change: Projections, Commitments

and Irreversibility. In: Climate Change 2013: The physical science basis. Contribution of working group I to the fifth assessment report of the intergovernmental panel on climate change. Cambridge University Press, Cambridge, United Kingdom and New York, NY, USA., pp 1029–1136 (2013)

Cowtan K, Hausfather Z, Hawkins E, et al. Robust comparison of climate models with observations using blended land air and ocean sea surface temperatures. *Geophys Res Lett* **42**, 6526–6534 (2015)

Dai A, Fyfe JC, Xie S-P, Dai X. Decadal modulation of global surface temperature by internal climate variability. *Nat Clim Chang* **5**, 555–559 (2015)

Dong L, Zhou T. The formation of the recent cooling in the eastern tropical Pacific Ocean and the associated climate impacts: A competition of global warming, IPO, and AMO. *J Geophys Res Atmos* **119**, 11272–11287 (2014)

Douville H, Voldoire A, Geoffroy O. The recent global warming hiatus: What is the role of Pacific variability? *Geophys Res Lett* **42**, 880–888 (2015)

England MH, Kajtar JB, Maher N. Robust warming projections despite the recent hiatus. *Nat Clim Chang* **5**, 394–396 (2015)

England MH, McGregor S, Spence P, et al. Recent intensification of wind-driven circulation in the Pacific and the ongoing warming hiatus. *Nat Clim Chang* **4**, 222–227 (2014)

Farneti R. Modelling interdecadal climate variability and the role of the ocean. *Wiley Interdiscip Rev Clim Chang* **8**, e441 (2017)

Flato G, Marotzke J, Abiodun B, et al. Evaluation of Climate Models. In: Climate Change 2013: The physical science basis. Contribution of working group I to the fifth assessment report of the intergovernmental panel on climate change. pp 741–866 (2013)

392 Frankcombe LM, England MH, Kajtar JB, et al. On the choice of ensemble mean for estimating
393 the forced signal in the presence of internal variability. *J Clim* **31**, 5681–5693 (2018)
394 Frankcombe LM, England MH, Mann ME, Steinman BA. Separating internal variability from
395 the externally forced climate response. *J Clim* **28**, 8184–8202 (2015)
396 GISTEMP Team. GISS Surface Temperature Analysis (GISTEMP).
397 http://www.data.giss.nasa.gov/gistemp/. Dataset accessed 2019-01-15. (2018)
398 Hansen JE, Ruedy R, Sato M, Lo K. Global surface temperature change. *Rev Geophys* **48**,
399 RG4004 (2010)
400 Hedemann C, Mauritsen T, Jungclaus JH, Marotzke J. The subtle origins of surface-warming
401 hiatuses. *Nat Clim Chang* **7**, 336–339 (2017)
402 Henley BJ, Gergis J, Karoly DJ, et al. A Tripole Index for the Interdecadal Pacific Oscillation.
403 *Clim Dyn* **45**, 3077–3090 (2015)
404 Henley BJ, King AD. Trajectories towards the 1.5°C Paris target: modulation by the Interdecadal
405 Pacific Oscillation. *Geophys Res Lett* **44**, 4256–4262 (2017)
406 Henley BJ, Meehl GA, Power SB, et al. Spatial and temporal agreement in climate model
407 simulations of the Interdecadal Pacific Oscillation. *Environ Res Lett* **12**, 044011 (2017)
408 Huang B, Angel W, Boyer T, et al. Evaluating SST analyses with independent ocean profile
409 observations. *J Clim* **31**, 5015–5030 (2018)
410 Huang B, Thorne PW, Banzon VF, et al. Extended Reconstructed Sea Surface Temperature
411 version 5 (ERSSTv5): Upgrades, Validations, and Intercomparisons. *J Clim* **30**, 8179–8205
412 (2017)
413 Huber M, Knutti R. Natural variability, radiative forcing and climate response in the recent
414 hiatus reconciled. *Nat Geosci* **7**, 651–656 (2014)

Kajtar JB, Santoso A, McGregor S, et al. Model under-representation of decadal Pacific trade wind trends and its link to tropical Atlantic bias. *Clim Dyn* **50**, 1471–1484 (2018)

Knight JR. The Atlantic Multidecadal Oscillation Inferred from the Forced Climate Response in Coupled General Circulation Models. *J Clim* **22**, 1610–1625 (2009)

Kosaka Y, Xie S-P. Recent global-warming hiatus tied to equatorial Pacific surface cooling. *Nature* **501**, 403–407 (2013)

Kosaka Y, Xie S-P. The tropical Pacific as a key pacemaker of the variable rates of global warming. *Nat Geosci* **9**, 669–673 (2016)

Li X-C, Xie S-P, Gille ST, Yoo C. Atlantic-induced pan-tropical climate change over the past three decades. *Nat Clim Chang* **6**, 275–279 (2016)

Luo J-J, Sasaki W, Masumoto Y. Indian Ocean warming modulates Pacific climate change. *Proc Natl Acad Sci* **109**, 18701–18706 (2012)

Lyu K, Yu J-Y. Climate impacts of the Atlantic Multidecadal Oscillation simulated in the CMIP5 models: A re-evaluation based on a revised index. *Geophys Res Lett* **44**, 3867–3876 (2017)

Maher N, Sen Gupta A, England MH. Drivers of decadal hiatus periods in the 20th and 21st centuries. *Geophys Res Lett* **41**, 5978–5986 (2014)

Mann ME, Steinman BA, Miller SK. On forced temperature changes, internal variability, and the AMO. *Geophys Res Lett* **41**, 3211–3219 (2014)

Marotzke J, Forster PM. Forcing, feedback and internal variability in global temperature trends. *Nature* **517**, 565–570 (2015)

McGregor S, Stuecker MF, Kajtar JB, England MH. Model tropical Atlantic biases underpin diminished Pacific decadal variability. *Nat Clim Chang* **8**, 493–498 (2018)

McGregor S, Timmermann A, Stuecker MF, et al. Recent Walker circulation strengthening and Pacific cooling amplified by Atlantic warming. *Nat Clim Chang* **4**, 888–892 (2014)

Medhaug I, Stolpe MB, Fischer EM, Knutti R. Reconciling controversies about the 'global warming hiatus.' *Nature* **545**, 41–47 (2017)

Meehl GA, Hu A, Santer BD, Xie S-P. Contribution of the Interdecadal Pacific Oscillation to twentieth-century global surface temperature trends. *Nat Clim Chang* **6**, 1005–1008 (2016)

Middlemas EA, Clement AC. Spatial patterns and frequency of unforced decadal-scale changes in global mean surface temperature in climate models. *J Clim* **29**, 6245–6257 (2016)

Morice CP, Kennedy JJ, Rayner NA, Jones PD. Quantifying uncertainties in global and regional temperature change using an ensemble of observational estimates: The HadCRUT4 data set. *J Geophys Res Atmos* **117**, D08101 (2012)

Murphy LN, Bellomo K, Cane MA, Clement AC. The Role of Historical Forcings in Simulating the Observed Atlantic Multidecadal Oscillation. *Geophys Res Lett* **44**, 2472–2480 (2017)

Nagy M, Petrovay K, Erdélyi R. The Atlanto-Pacific multidecade oscillation and its imprint on the global temperature record. *Clim Dyn* **48**, 1883–1891 (2017)

Newman M, Alexander MA, Ault TR, et al. The Pacific Decadal Oscillation, revisited. *J Clim* **29**, 4399–4427 (2016)

O'Reilly CH, Huber M, Woollings T, Zanna L. The signature of low-frequency oceanic forcing in the Atlantic Multidecadal Oscillation. *Geophys Res Lett* **43**, 2810–2818 (2016)

Oka A, Watanabe M. The post-2002 global surface warming slowdown caused by the subtropical Southern Ocean heating acceleration. *Geophys Res Lett* **44**, 3319–3327 (2017)

Palmer MD, McNeall DJ. Internal variability of Earth's energy budget simulated by CMIP5 climate models. *Environ Res Lett* **9**, 034016 (2014)

Pasini A, Triacca U, Attanasio A. Evidence for the role of the Atlantic multidecadal oscillation and the ocean heat uptake in hiatus prediction. *Theor Appl Climatol* **129**, 873–880 (2017)

Rayner NA, Parker DE, Horton EB, et al. Global analyses of sea surface temperature, sea ice, and night marine air temperature since the late nineteenth century. *J Geophys Res* **108**, ACL-2 (2003)

Riahi K, Rao S, Krey V, et al. RCP 8.5-A scenario of comparatively high greenhouse gas emissions. *Clim Change* **109**, 33–57 (2011)

Santer BD, Bonfils C, Painter JF, et al. Volcanic contribution to decadal changes in tropospheric temperature. *Nat Geosci* **7**, 185–189 (2014)

Schmidt GA, Shindell DT, Tsigaridis K. Reconciling warming trends. *Nat Geosci* **7**, 158–160 (2014)

Schurer AP, Hegerl GC, Mann ME, et al. Separating forced from chaotic climate variability over the past millennium. *J Clim* **26**, 6954–6973 (2013)

Sen Gupta A, Jourdain NC, Brown JN, Monselesan DP. Climate drift in the CMIP5 models. *J Clim* **26**, 8597–8615 (2013)

Smith DM, Booth BBB, Dunstone NJ, et al. Role of volcanic and anthropogenic aerosols in the recent global surface warming slowdown. *Nat Clim Chang* **6**, 936–940 (2016)

Steinman BA, Mann ME, Miller SK. Atlantic and Pacific multidecadal oscillations and Northern Hemisphere temperatures. *Science* **347**, 2269–2272 (2015)

Stolpe MB, Medhaug I, Knutti R. Contribution of Atlantic and Pacific Multidecadal Variability to Twentieth Century Temperature Changes. *J Clim* **30**, 6279–6295 (2017)

Trenberth KE, Shea DJ. Atlantic hurricanes and natural variability in 2005. *Geophys Res Lett* **33**, L12704 (2006)

Vecchi GA, Delworth TL, Booth BBB. Climate Science: Origins of Atlantic decadal swings. *Nature* **548**, 284–285 (2017)

Vernier JP, Thomason LW, Pommereau JP, et al. Major influence of tropical volcanic eruptions on the stratospheric aerosol layer during the last decade. *Geophys Res Lett* **38**, L12807 (2011)

Wang J, Yang B, Ljungqvist FC, et al. Internal and external forcing of multidecadal Atlantic climate variability over the past 1,200 years. *Nat Geosci* **10**, 512–517 (2017)

Watanabe M, Shiogama H, Tatebe H, et al. Contribution of natural decadal variability to global warming acceleration and hiatus. *Nat Clim Chang* **4**, 893–897 (2014)

Yan X, Zhang R, Knutson TR. Underestimated AMOC variability and implications for AMV and predictability in CMIP models. *Geophys Res Lett* **45**, 4319–4328 (2018)

Yao S-L, Huang G, Wu R, Qu X. The global warming hiatus—a natural product of interactions of a secular warming trend and a multi-decadal oscillation. *Theor Appl Climatol* **123**, 349–360 (2016)

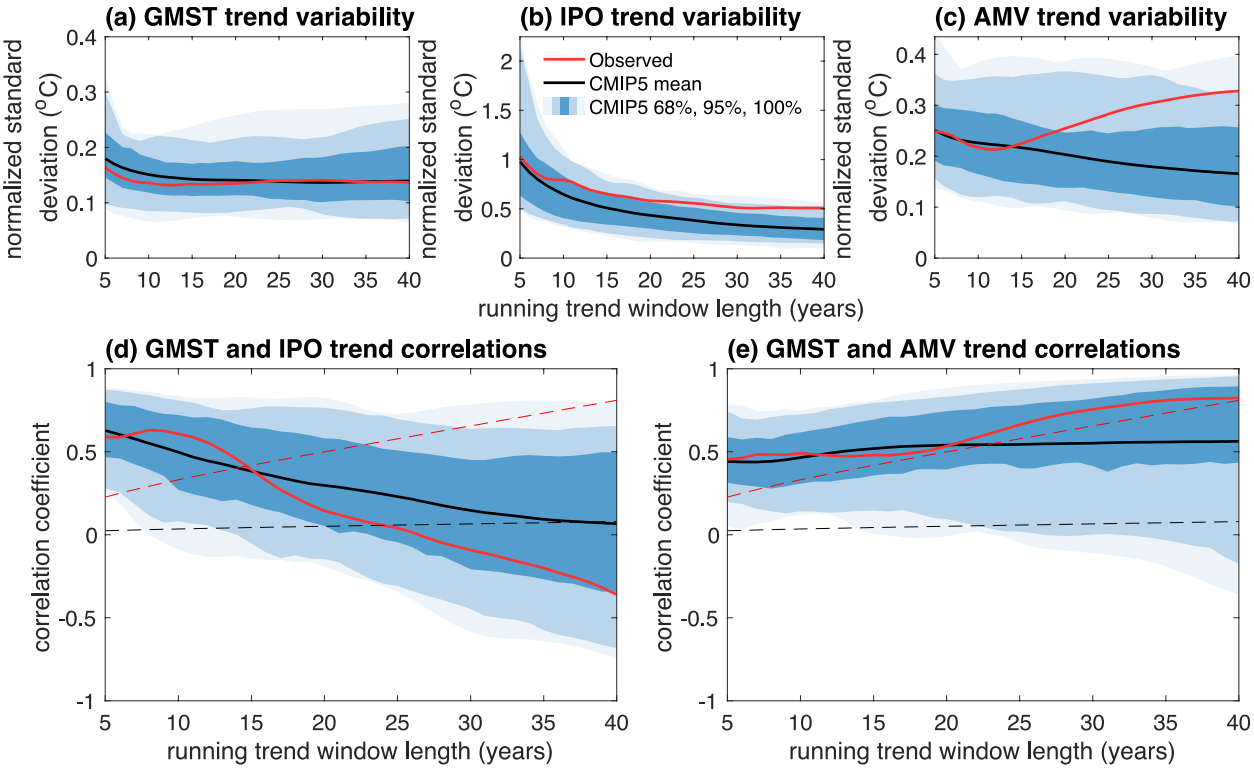

504

505 **Figure 1.** Standard deviation and correlations in the running trends of global mean surface
506 temperature (GMST), the Interdecadal Pacific Oscillation (IPO), and the Atlantic Multidecadal
507 Variability (AMV) indices. **(a-c)** Standard deviation of running trend data, using a range of
508 window lengths, for **(a)** GMST, **(b)** the IPO index, and **(c)** the AMV index, in observations and
509 CMIP5 historical simulations. The shaded blue regions denote the central 68%, 95%, and 100%
510 of the CMIP5 individual realization ensemble. For example, the darkest blue indicates the spread
511 of the central 68% of realizations (more specifically, 59 out of 87 realizations). To better
512 illustrate the variability on a linear y-axis scale, the standard deviation was normalized by
513 multiplying it with the running window length (in years), and hence the units are °C. **(d, e)**
514 Correlations in running trends of GMST with **(d)** the IPO index and **(e)** the AMV index, using a
515 range of window lengths. Dashed lines denote the 95% levels for statistically significant
516 correlations (Text S3) for the observed data (red) and model data (black).

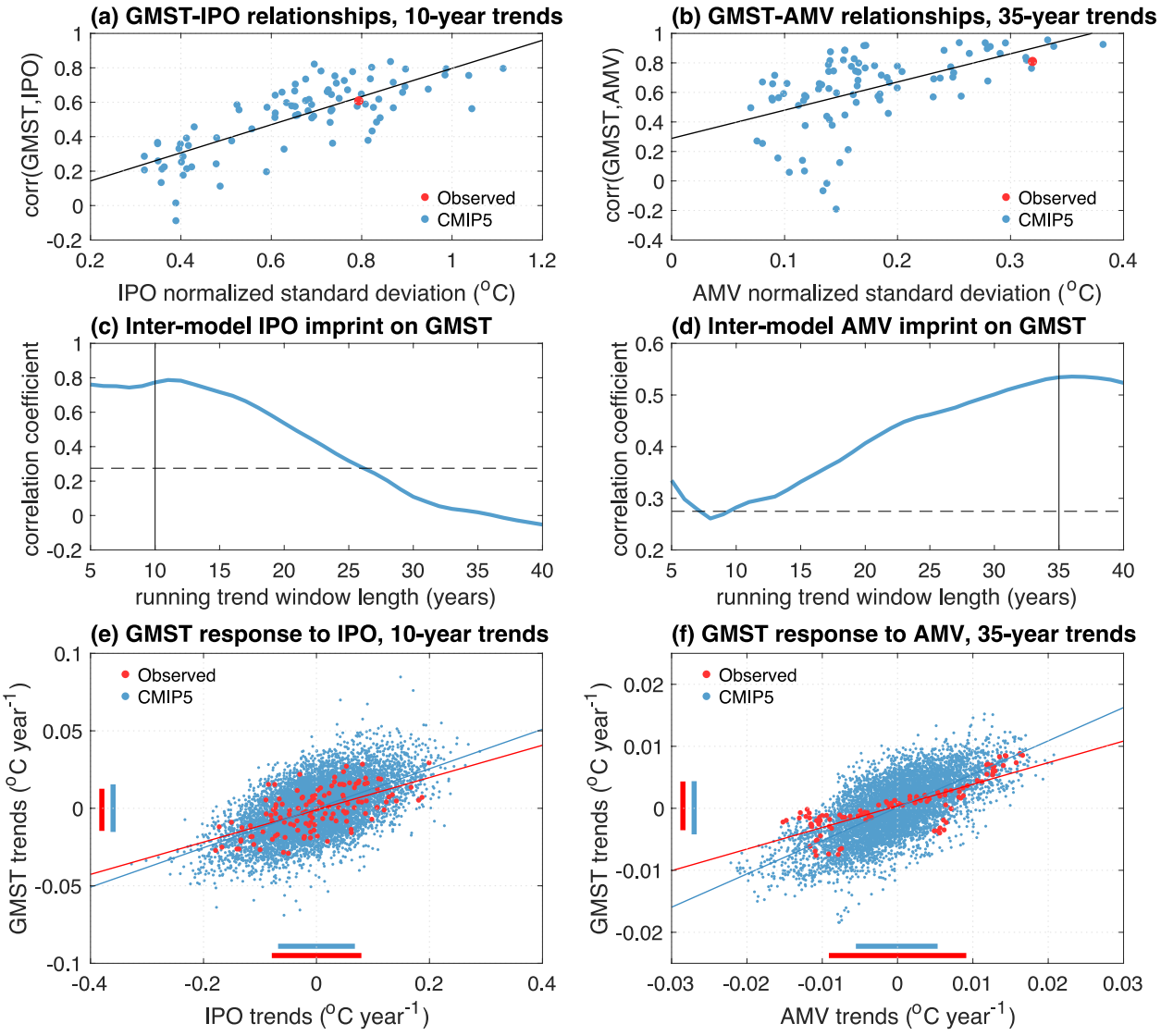

Figure 2. Relationships between running trends of global mean surface temperature (GMST), the Interdecadal Pacific Oscillation (IPO), and the Atlantic Multidecadal Variability (AMV) indices. **(a)** Relationship between the normalized standard deviation of the 10-year running trend in IPO index (Figure 1b), and the correlation between 10-year running trends of GMST and IPO index (Figure 1d). **(b)** As in **(a)**, but for 35-year running trends of GMST and AMV index (Figure 1c,e). **(c)** The CMIP5 inter-model correlations of IPO standard deviation against GMST-IPO running trend correlations. For a given running trend window length, *N*, the y-axis value denotes the correlation between two data sets: (i) the normalized standard deviation of the *N*-year running

trend of IPO index in each CMIP5 realization, and (ii) the correlation between *N*-year running trends of GMST and IPO index. For example, the vertical black line denotes the window length selected in **(a)**, and thus the value of 0.77 for 10-year trends denotes the correlation computed for the CMIP5 data in **(a)**. The dashed line denotes the 99% levels for statistically significant inter-model correlations. **(d)** The CMIP5 inter-model correlations of AMV against GMST-AMV running trend correlations. The vertical black line denotes the window length selected in **(b)**, and thus the value of 0.53 for 35-year trends denotes the correlation computed for the CMIP5 data in **(b)**. **(e)** Response of 10-year GMST trends to 10-year IPO index trends, in all CMIP5 historical realizations, and observations. The red (observed) and blue (CMIP5) lines denote the ordinary least squares fits to the data. The red (observed) and blue (CMIP5) horizontal and vertical bars denote the one standard deviation ranges in the data. **(f)** As in **(e)**, but for 35-year trends in GMST and AMV index.

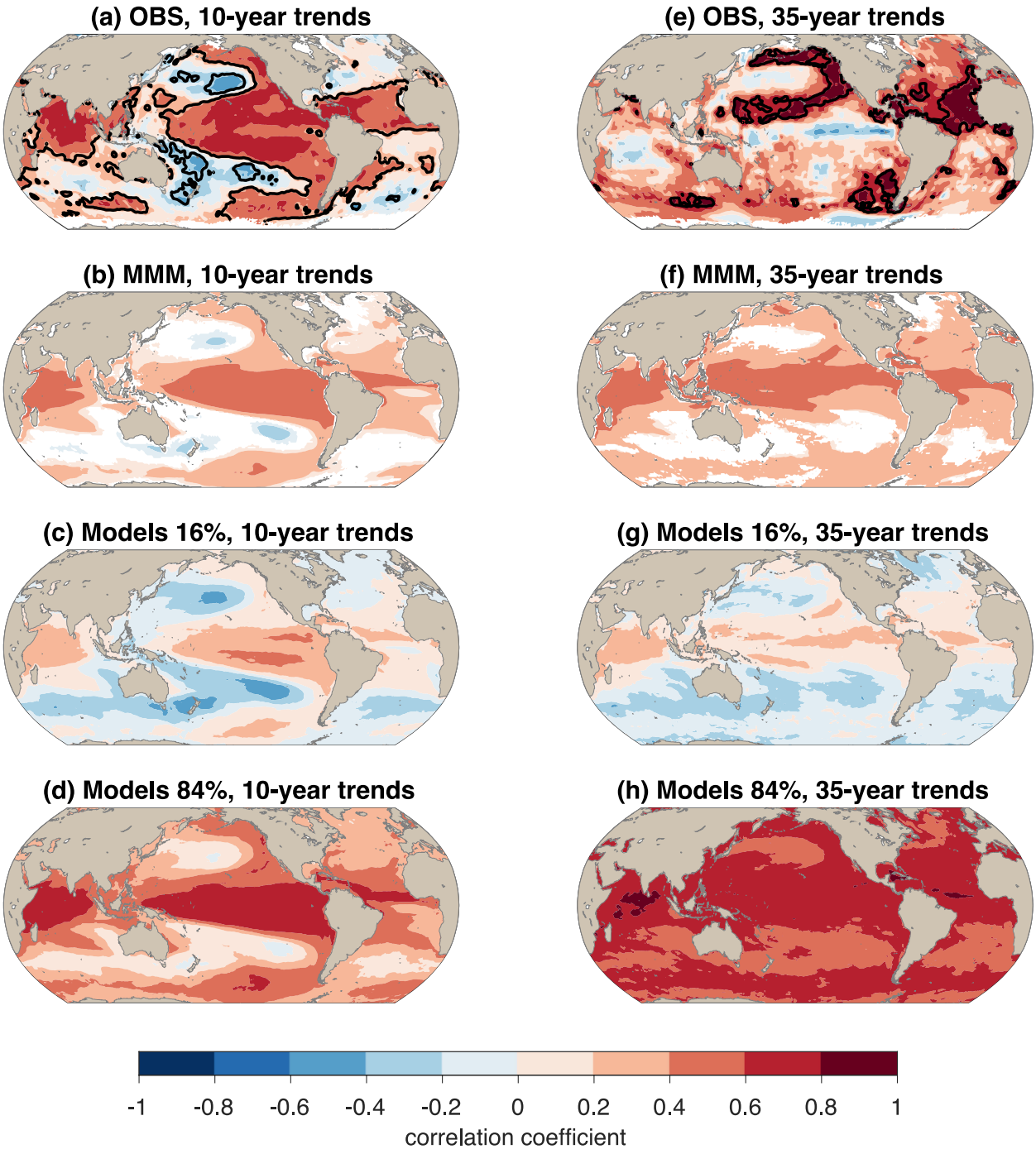

Figure 3. Correlations between running trends of global mean surface temperature (GMST) and grid-point sea surface temperature (SST). **(a-d)** 10-year running trends, and **(e-h)** 35-year running trends, for **(a,e)** observations, **(b,f)** the multi-model mean (MMM) of the CMIP5 historical correlations, **(c,g)** the 16th percentile, at each grid-point, of the correlations from the

CMIP5 historical realization set, and **(d,h)** the 84th percentile. The forced response was first removed from GMST and from each SST grid-point. For the observed data **(a,e)**, the 95% statistical significance levels for correlations are indicated by black contours (Text S3). For the multi-model mean data **(b,f)**, correlations are plotted only where at least 75% of the models agree on the sign.

Figure 1.

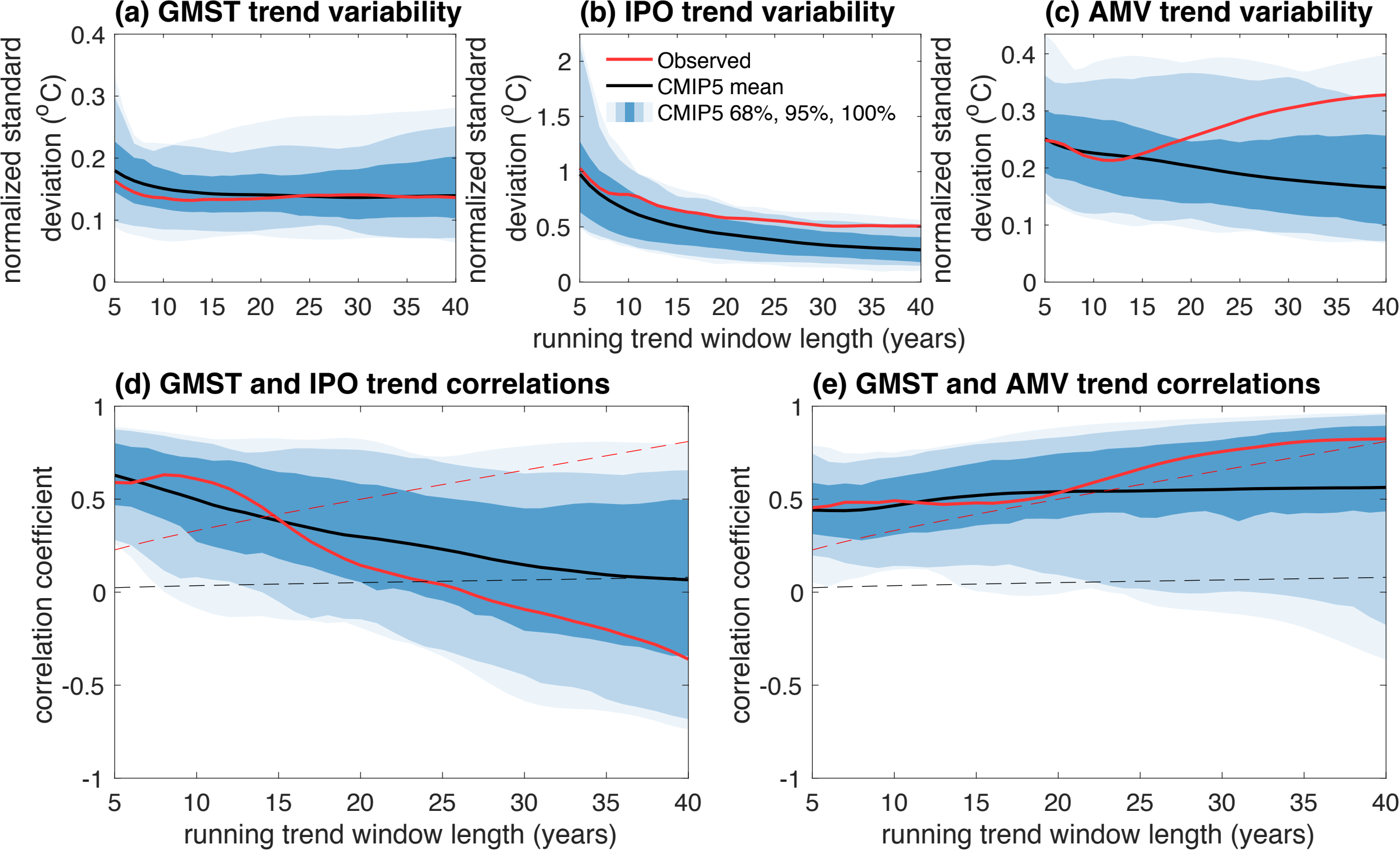
(a) GMST trend variability
(b) IPO trend variability
(c) AMV trend variability
normalized standard deviation (°C)
Observed
CMIP5 mean
CMIP5 68%, 95%, 100%
running trend window length (years)
(d) GMST and IPO trend correlations
(e) GMST and AMV trend correlations
correlation coefficient

Figure 2.

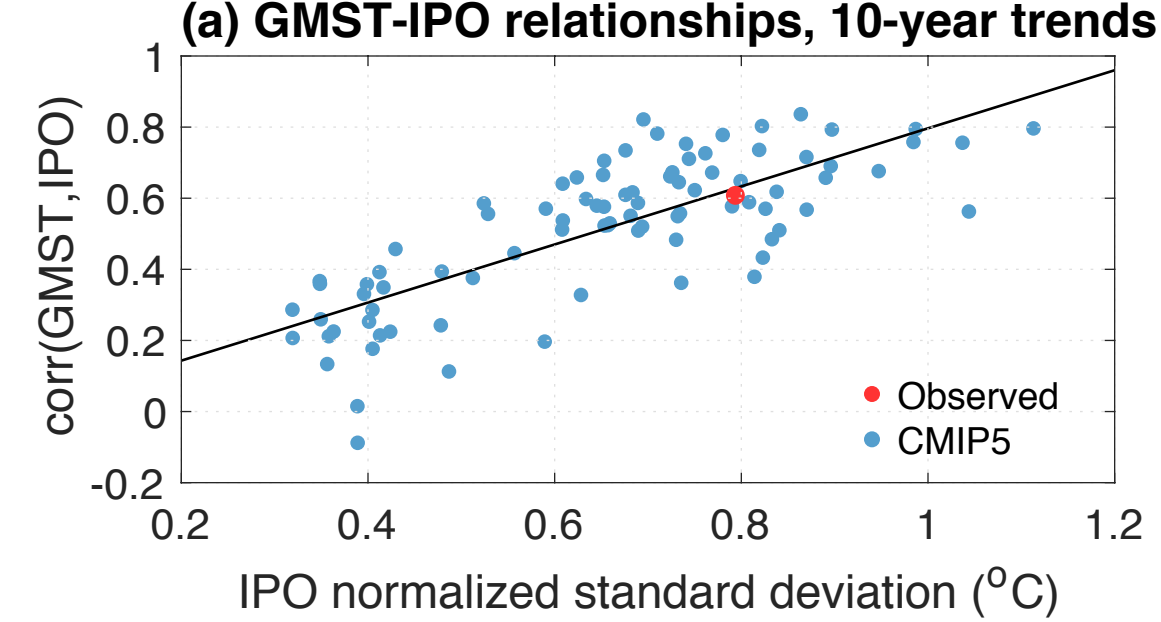
(a) GMST-IPO relationships, 10-year trends
corr(GMST,IPO)
IPO normalized standard deviation (°C)
Observed
CMIP5

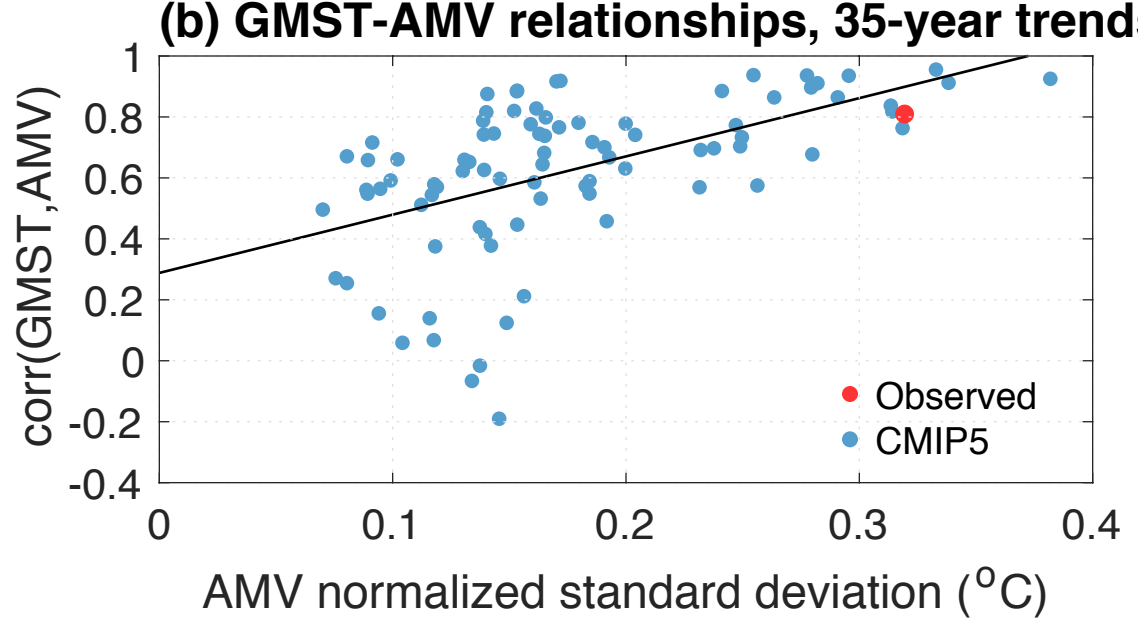
(b) GMST-AMV relationships, 35-year trends
corr(GMST,AMV)
AMV normalized standard deviation (°C)
Observed
CMIP5

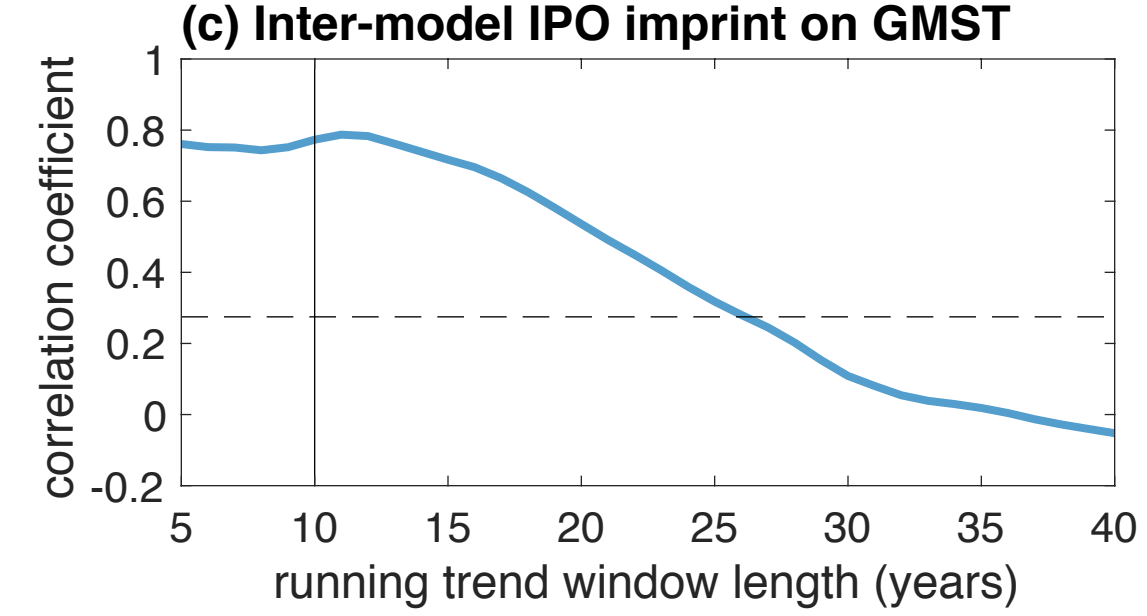
(c) Inter-model IPO imprint on GMST
correlation coefficient
running trend window length (years)

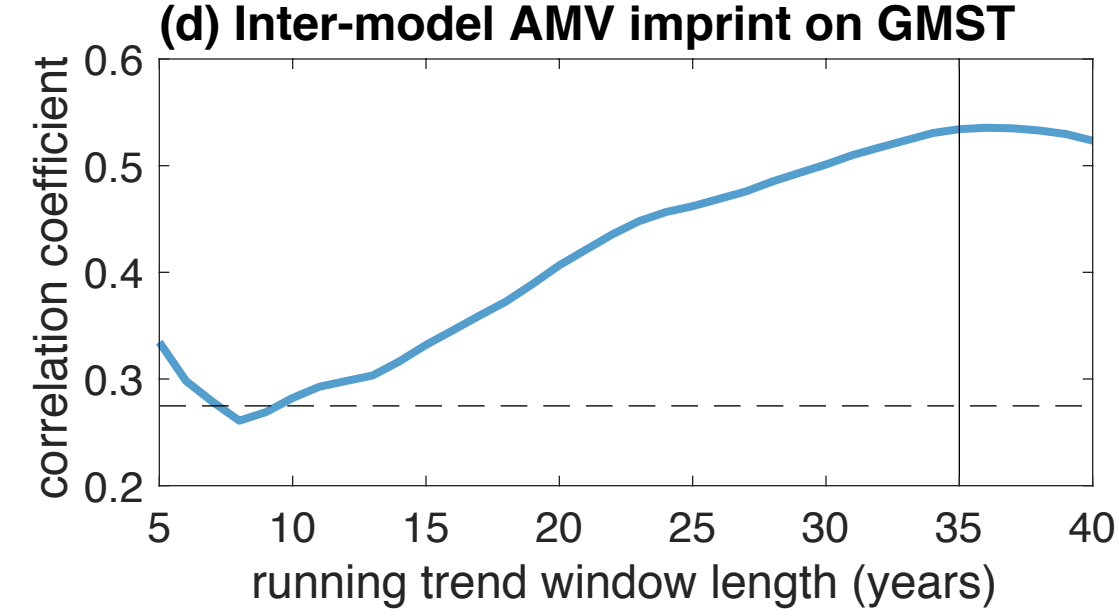
(d) Inter-model AMV imprint on GMST
correlation coefficient
running trend window length (years)

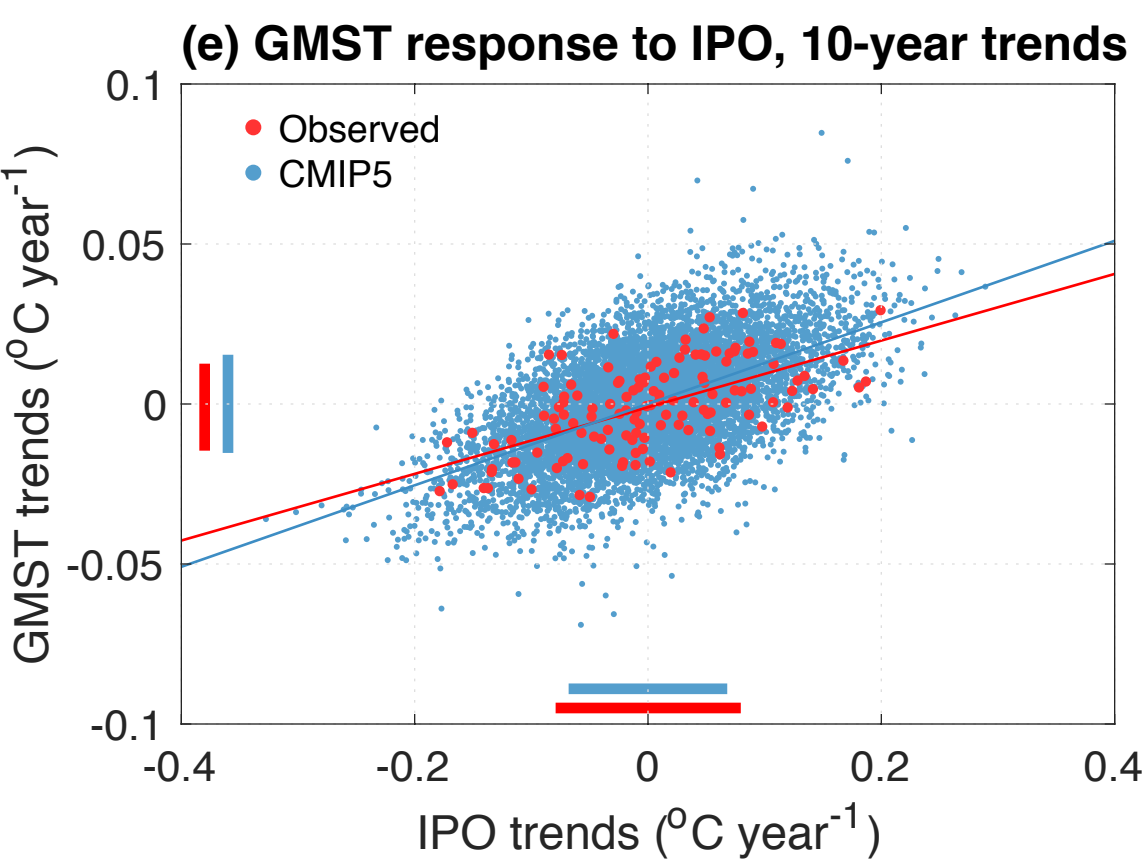
(e) GMST response to IPO, 10-year trends
GMST trends (°C year-1)
IPO trends (°C year-1)
Observed
CMIP5

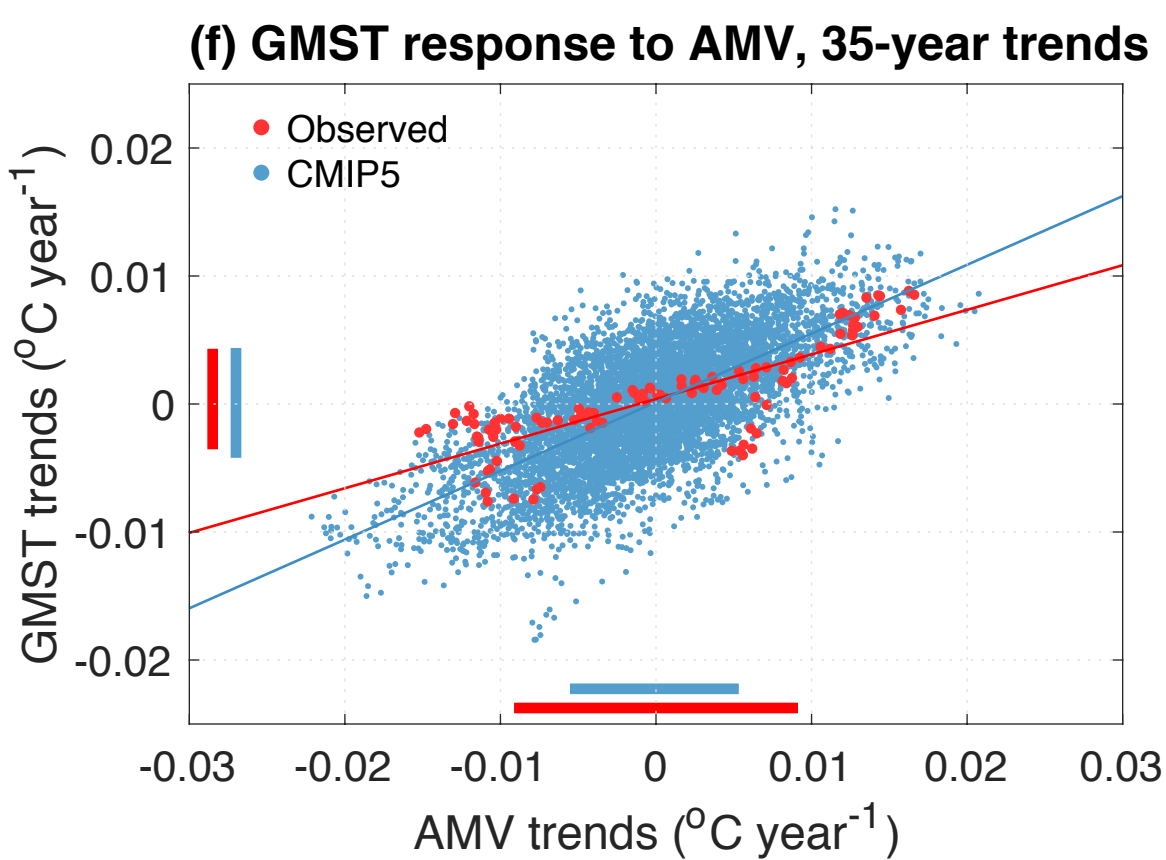
(f) GMST response to AMV, 35-year trends
GMST trends (°C year-1)
AMV trends (°C year-1)
Observed
CMIP5

Figure 3.

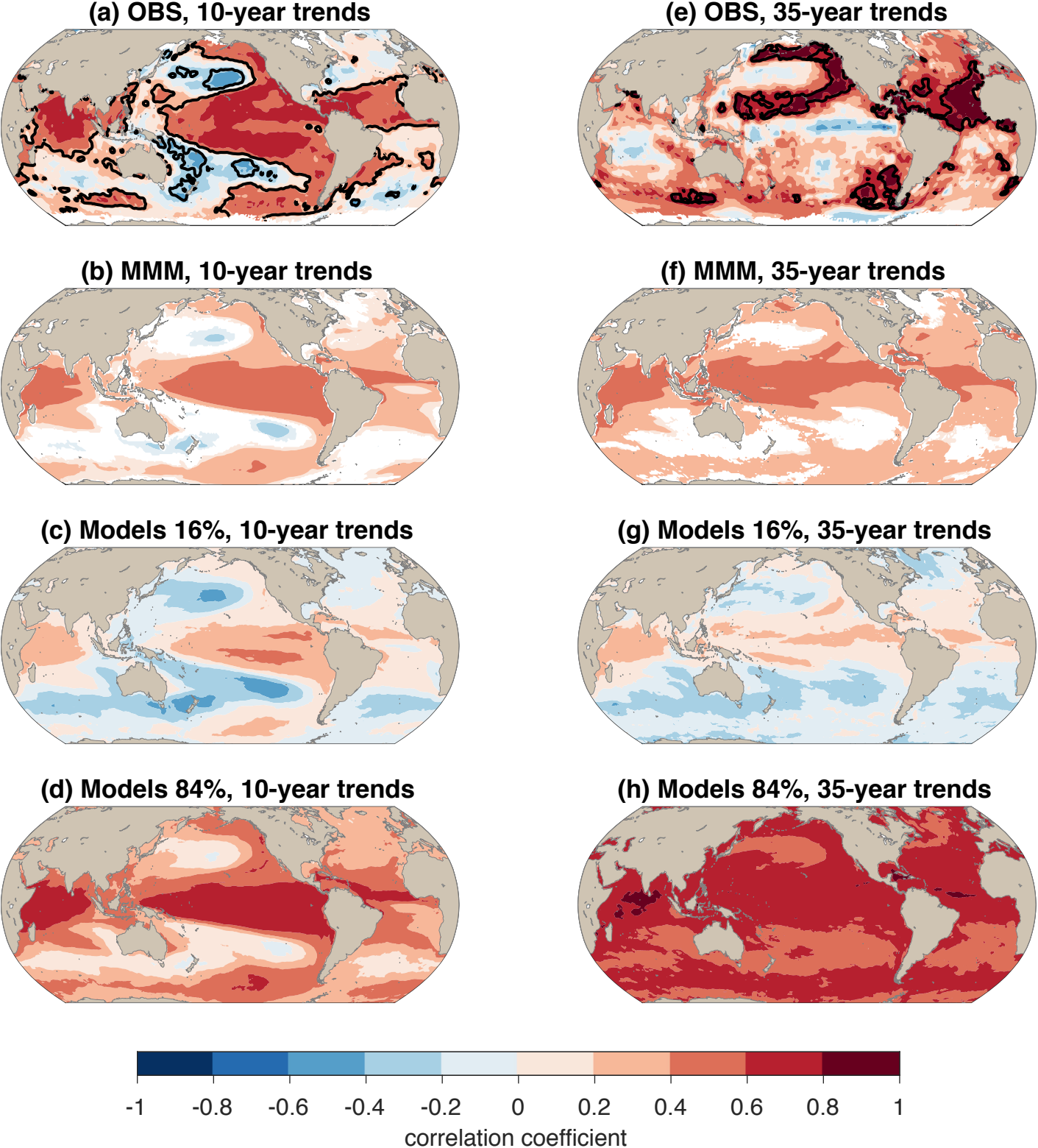
(a) OBS, 10-year trends
(e) OBS, 35-year trends
(b) MMM, 10-year trends
(f) MMM, 35-year trends
(c) Models 16%, 10-year trends
(g) Models 16%, 35-year trends
(d) Models 84%, 10-year trends
(h) Models 84%, 35-year trends
-1
-0.8
-0.6
-0.4
-0.2
0
0.2
0.4
0.6
0.8
1
correlation coefficient